Basics of Fourier Analysis

1.1 FORWARD AND INVERSE FOURIER TRANSFORM

Fourier transform (FT) is a common and useful mathematical tool that is utilized in numerous applications in science and technology. FT is quite practical, especially for characterizing nonlinear functions in nonlinear systems, analyzing random signals, and solving linear problems. FT is also a very important tool in radar imaging applications as we shall investigate in the forthcoming chapters of this book. Before starting to deal with the FT and inverse Fourier transform (IFT), a brief history of this useful linear operator and its founders is presented.

1.1.1 Brief History of FT

Jean Baptiste Joseph Fourier, a great mathematician, was born in 1768 in Auxerre, France. His special interest in heat conduction led him to describe a mathematical series of sine and cosine terms that can be used to analyze propagation and diffusion of heat in solid bodies. In 1807, he tried to share his innovative ideas with researchers by preparing an essay entitled "On the Propagation of Heat in Solid Bodies." The work was examined by Lagrange, Laplace, Monge, and Lacroix. Lagrange's oppositions caused the rejection of Fourier's paper. This unfortunate decision caused colleagues to wait for 15 more years to read his remarkable contributions on mathematics, physics, and, especially, signal analysis. Finally, his ideas were published in the book *The Analytic Theory of Heat* in 1822 [1].

Discrete Fourier transform (DFT) was developed as an effective tool in calculating this transformation. However, computing FT with this tool in the

19th century was taking a long time. In 1903, Carl Runge studied the minimization of the computational time of the transformation operation [2]. In 1942, Danielson and Lanczos utilized the symmetry properties of FT to reduce the number of operations in DFT [3]. Before the advent of digital computing technologies, James W. Cooley and John W. Tukey developed a fast method to reduce the computation time in DFT. In 1965, they published their technique that later on became famous as the fast Fourier transform (FFT) [4].

1.1.2 Forward FT Operation

The FT can be simply defined as a certain linear operator that maps functions or signals defined in one domain to other functions or signals in another domain. The common use of FT in electrical engineering is to transform signals from time domain to frequency domain or vice versa. More precisely, forward FT decomposes a signal into a continuous spectrum of its frequency components such that the time signal is transformed to a frequency-domain signal. In radar applications, these two opposing domains are usually represented as "spatial frequency" (or wave number) and "range" (distance). Such use of FT will be examined and applied throughout this book.

The forward FT of a continuous signal $g(t)$ where $-\infty < t < \infty$ is described as

$$
\begin{aligned}
G(f) &= \mathcal{F}\{g(t)\} \\
&= \int_{-\infty}^{\infty} g(t) \cdot e^{-j2\pi ft} dt.
\end{aligned}
\tag{1.1}
$$

To appreciate the meaning of FT, the multiplying function $e^{-j2\pi ft}$ and operators (multiplication and integration) on the right side of Equation 1.1 should be investigated carefully: The term $e^{-j2\pi f_i t}$ is a complex phasor representation for a sinusoidal function with the single frequency of f_i. This signal oscillates only at the frequency of f_i and does not contain any other frequency component. Multiplying the signal in interest, $g(t)$, with the term $e^{-j2\pi f_i t}$ provides the similarity between each signal, that is, how much of $g(t)$ has the frequency content of f_i. Integrating this multiplication over all time instances from $-\infty$ to ∞ will sum the f_i contents of $g(t)$ over all time instants to give $G(f_i)$; that is, the amplitude of the signal at the particular frequency of f_i. Repeating this process for all the frequencies from $-\infty$ to ∞ will provide the frequency spectrum of the signal; that is, $G(f)$. Therefore, the transformed signal represents the continuous spectrum of frequency components; that is, representation of the signal in "frequency domain."

1.1.3 IFT

This transformation is the inverse operation of the FT. IFT, therefore, synthesizes a frequency-domain signal from its spectrum of frequency components

to its time-domain form. The IFT of a continuous signal $G(f)$ where $-\infty < f < \infty$ is described as

$$g(t) = \mathcal{F}^{-1}\{G(f)\}$$
$$= \int_{-\infty}^{\infty} G(f) \cdot e^{j2\pi ft} df. \tag{1.2}$$

1.2 FT RULES AND PAIRS

There are many useful Fourier transform rules and pairs that can be very helpful when applying the FT or IFT to different real-world applications. We will briefly revisit them to remind the reader of the properties of FT. Provided that FT and IFT are defined as in Equations 1.1 and 1.2, respectively, FT pair is denoted as

$$g(t) \overset{\mathcal{F}}{\leftrightarrow} G(f), \tag{1.3}$$

where $\mathcal{F}$ represents the forward FT operation from time domain to frequency domain. The IFT operation is represented by $\mathcal{F}^{-1}$ and the corresponding alternative pair is given by

$$G(f) \overset{\mathcal{F}^{-1}}{\leftrightarrow} g(t). \tag{1.4}$$

Here, the transformation is from frequency domain to time domain. Based on these notations, the properties of FT are listed briefly below.

1.2.1 Linearity

If $G(f)$ and $H(f)$ are the FTs of the time signals $g(t)$ and $h(t)$, respectively, the following equation is valid for the scalars a and b:

$$a \cdot g(t) + b \cdot h(t) \overset{\mathcal{F}}{\leftrightarrow} a \cdot G(f) + b \cdot H(f). \tag{1.5}$$

Therefore, the FT is a linear operator.

1.2.2 Time Shifting

If the signal is shifted in time with a value of t_o, then its frequency domain signal is multiplied with a phase term as listed below:

$$g(t - t_o) \overset{\mathcal{F}}{\leftrightarrow} e^{-j2\pi ft_o} \cdot G(f) \tag{1.6}$$

1.2.3   Frequency Shifting

If the time signal is multiplied by a phase term of $e^{j2\pi f_o t}$, then the FT of this time signal is shifted in frequency by f_o:

$$e^{j2\pi f_o t} \cdot g(t) \overset{\mathcal{F}}{\leftrightarrow} G(f - f_o) \tag{1.7}$$

1.2.4   Scaling

If the time signal is scaled by a constant a, then the spectrum is also scaled with the following rule:

$$g(at) \overset{\mathcal{F}}{\leftrightarrow} \frac{1}{|a|} G\left(\frac{f}{a}\right), \quad a \in \mathbb{R}, \, a \neq 0. \tag{1.8}$$

1.2.5   Duality

If the spectrum signal $G(f)$ is taken as a time signal $G(t)$, then the corresponding frequency-domain signal will be the time reversal equivalent of the original time-domain signal, $g(t)$:

$$G(t) \overset{\mathcal{F}}{\leftrightarrow} g(-f). \tag{1.9}$$

1.2.6   Time Reversal

If the time is reversed for the time-domain signal, then the frequency is also reversed in the frequency-domain signal:

$$g(-t) \overset{\mathcal{F}}{\leftrightarrow} G(-f). \tag{1.10}$$

1.2.7   Conjugation

If the conjugate of the time-domain signal is taken, then the frequency-domain signal is conjugated and frequency-reversed:

$$g^*(t) \overset{\mathcal{F}}{\leftrightarrow} G^*(-f). \tag{1.11}$$

1.2.8   Multiplication

If the time-domain signals $g(t)$ and $h(t)$ are multiplied in time, then their spectrum signals $G(f)$ and $H(f)$ are convolved in frequency:

$$g(t) \cdot h(t) \overset{\mathcal{F}}{\leftrightarrow} G(f) * H(f). \tag{1.12}$$

1.2.9 Convolution

If the time-domain signals $g(t)$ and $h(t)$ are convolved in time, then their spectrum signals $G(f)$ and $H(f)$ are multiplied in the frequency domain:

$$g(t)*h(t)\overset{\mathcal{F}}{\leftrightarrow}G(f)\cdot H(f). \tag{1.13}$$

1.2.10 Modulation

If the time-domain signal is modulated with sinusoidal functions, then the frequency-domain signal is shifted by the amount of the frequency at that particular sinusoidal function:

$$g(t)*cos(2\pi f_o t)\overset{\mathcal{F}}{\leftrightarrow}\frac{1}{2}(G(f+f_o)+G(f-f_o))$$

$$g(t)*sin(2\pi f_o t)\overset{\mathcal{F}}{\leftrightarrow}\frac{j}{2}(G(f+f_o)-G(f-f_o)). \tag{1.14}$$

1.2.11 Derivation and Integration

If the derivative or integration of a time-domain signal is taken, then the corresponding frequency-domain signal is given as below:

$$\frac{d}{dt}g(t)\overset{\mathcal{F}}{\leftrightarrow}2\pi f\cdot G(f)$$

$$\int_{-\infty}^{t}g(\tau)d\tau\overset{\mathcal{F}}{\leftrightarrow}\frac{1}{j2\pi f}G(f)+\pi G(0)\cdot\delta(f). \tag{1.15}$$

1.2.12 Parseval's Relationship

A useful property that was claimed by Parseval is that since the FT (or IFT) operation maps a signal in one domain to another domain, the signals' energies should be exactly the same as given by the following relationship:

$$\int_{-\infty}^{\infty}|g(t)|^2\,dt\overset{\mathcal{F}}{\leftrightarrow}\int_{-\infty}^{\infty}|G(f)|^2\,df. \tag{1.16}$$

1.3 TIME-FREQUENCY REPRESENTATION OF A SIGNAL

While the FT concept can be successfully utilized for the stationary signals, there are many real-world signals whose frequency contents vary over time. To be able to display these frequency variations over time, joint time-frequency (JTF) transforms/representations are used.
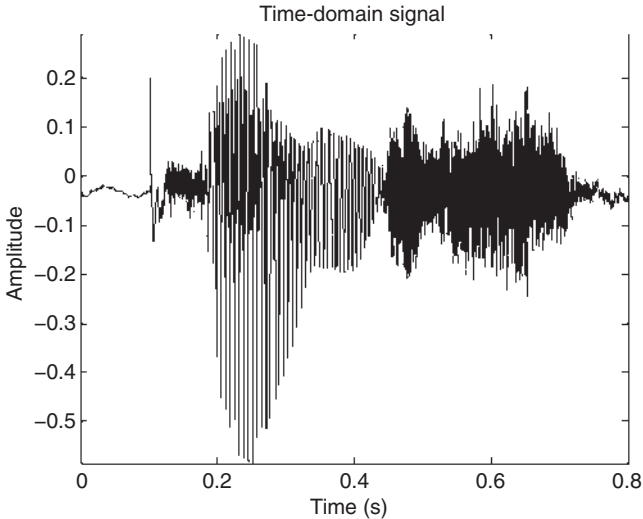
FIGURE 1.1   The time-domain signal of "prince" spoken by a lady.

1.3.1   Signal in the Time Domain

The term "time domain" is used while describing functions or physical signals with respect to time either continuous or discrete. The time-domain signals are usually more comprehensible than the frequency-domain signals since most of the real-world signals are recorded and displayed versus time. A common equipment to analyze time-domain signals is the *oscilloscope*. In Figure 1.1, a time-domain sound signal is shown. This signal is obtained by recording an utterance of the word "prince" by a lady [5]. By looking at the occurrence instants in the x-axis and the signal magnitude in the y-axis, one can analyze the stress of the letters in the word "prince."

1.3.2   Signal in the Frequency Domain

The term "frequency domain" is used while describing functions or physical signals with respect to frequency either continuous or discrete. Frequency-domain representation has been proven to be very useful in numerous engineering applications while characterizing, interpreting, and identifying signals. Solving differential equations and analyzing circuits and signals in communication systems are a few applications among many others where frequency-domain representation is much more advantageous than time-domain representation. The frequency-domain signal is traditionally obtained by taking the FT of the time-domain signal. As briefly explained in Section 1.1, FT is generated by expressing the signal onto a set of basis functions, each of which is a sinusoid with the unique frequency. Displaying the measure of the similarities of the original time-domain signal to those particular unique
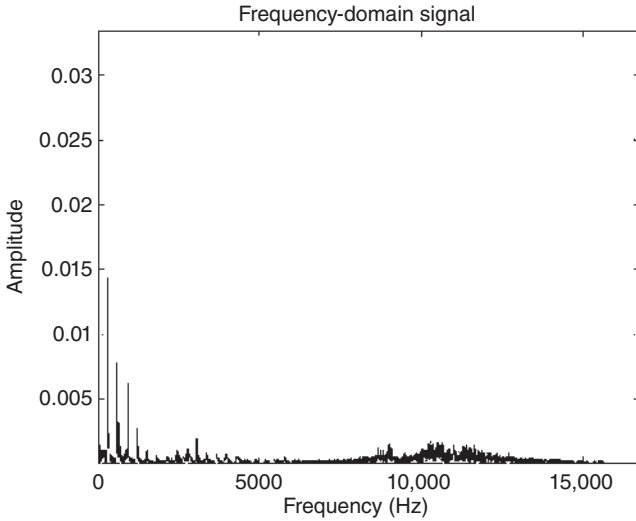
FIGURE 1.2   The frequency-domain signal (or the spectrum) of "prince."

frequency bases generates the Fourier transformed signal, or the frequency-domain signal. Spectrum analyzers and network analyzers are the common equipment which analyze frequency-domain signals. These signals are not as quite perceivable when compared to time-domain signals. In Figure 1.2, the frequency-domain version of the sound signal in Figure 1.1 is obtained by using the FT operation. The signal intensity value at each frequency component can be read from the y-axis. The frequency content of a signal is also called the spectrum of that signal.

1.3.3   Signal in the (JTF) Plane

Although FT is very effective for demonstrating the frequency content of a signal, it does not give the knowledge of frequency variation over time. However, most of the real-world signals have time-varying frequency content such as speech and music signals. In these cases, the single-frequency sinusoidal bases are not suitable for the detailed analysis of those signals. Therefore, JTF analysis methods were developed to represent these signals both in time and frequency to observe the variation of frequency content as the time progresses.

There are many tools to map a time-domain or frequency-domain signal onto the JTF plane. Some of the most well-known JTF tools are the short-time Fourier transform (STFT) [6], the Wigner–Ville distribution [7], the Choi-Willams distribution [8], the Cohen's class [9], and the time-frequency distribution series (TFDS) [10]. Among these, the most appreciated and commonly used is the STFT or the spectrogram. The STFT can easily display the

variations in the sinusoidal frequency and phase content of local moments of a signal over time with sufficient resolution in most cases.

The spectrogram transforms the signal onto two-dimensional (2D) time-frequency plane via the following famous equation:

$$STFT\{g(t)\} \triangleq G(t,f)$$
$$= \int_{-\infty}^{\infty} g(\tau) \cdot w(\tau - t) e^{-j2\pi f\tau} d\tau. \tag{1.17}$$

This transformation formula is nothing but the short-time (or short-term) version of the famous FT operation defined in Equation 1.1. The main signal, $g(t)$, is multiplied with a shorter duration window signal, $w(t)$. By sliding this window signal over $g(t)$ and taking the FT of the product, only the frequency content for the windowed version of the original signal is acquired. Therefore, after completing the sliding process over the whole duration of the time-domain signal $g(t)$ and putting corresponding FTs side by side, the final 2D STFT of $g(t)$ is obtained.

It is obvious that STFT will produce different output signals for different duration windows. The duration of the window affects the resolutions in both domains. While a very short-duration time window provides a good resolution in the time domain, the resolution in the frequency domain becomes poor. This is because of the fact that the time duration and the frequency bandwidth of a signal are inversely proportional to each other. Similarly, a long duration time signal will give a good resolution in the frequency domain while the resolution in the time domain will be bad. Therefore, a reasonable compromise has to be attained about the duration of the window in time to be able to view both domains with fairly good enough resolutions.

The shape of the window function has an effect on the resolutions as well. If a window function with sharp ends is chosen, there will be strong sidelobes in the other domain. Therefore, smooth waveform type windows are usually utilized to obtain well-resolved images with less sidelobes with the price of increased main lobe beamwidth; that is, less resolution. Commonly used window types are Hanning, Hamming, Kaiser, Blackman, and Gaussian.

An example of the use of spectrograms is demonstrated in Figure 1.3. The spectrogram of the sound signal in Figure 1.1 is obtained by applying the STFT operation with a Hanning window. This JTF representation obviously demonstrates the frequency content of different syllables when the word "prince" is spoken. Figure 1.3 illustrates that while the frequency content of the part "prin . . ." takes place at low frequencies, that of the part ". . . ce" occurs at much higher frequencies.

JTF transformation tools have been found to be very useful in interpreting the physical mechanisms such as scattering and resonance for radar applications [11–14]. In particular, when JTF transforms are used to form the 2D image of electromagnetic scattering from various structures, many useful physical features can be displayed. Distinct time events (such as scattering from
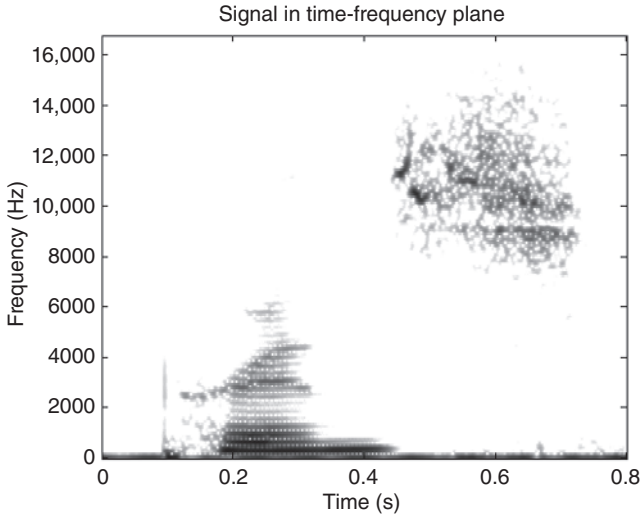
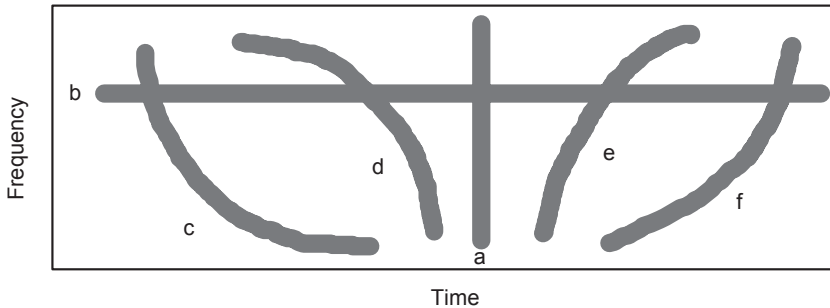**FIGURE 1.3**   The time-frequency representation of the word "prince."

FIGURE 1.4   Images of scattering mechanisms in the joint time-frequency plane: (a) scattering center, (b) resonance, (c and d) dispersion due to material, (e and f) dispersion due to geometry of the structure.

point targets or specular points) show up as vertical line in the JTF plane as depicted in Figure 1.4a. Therefore, these scattering centers appear at only one time instant but for all frequencies. A resonance behavior such as scattering from an open cavity structure shows up as horizontal line on the JTF plane. Such mechanisms occur only at discrete frequencies but over all time instants (see Fig. 1.4b). Dispersive mechanisms, on the other hand, are represented on the JTF plane as slanted curves. If the dispersion is due to the material, then the slope of the image is positive as shown in Figure 1.4c,d. The dielectric coated structures are the good examples of this type of dispersion. The reason

for having a slanted line is because of the modes excited inside such materials. As frequency increases, the wave velocity changes for different modes inside these materials. Consequently, these modes show up as slanted curves in the JTF plane. Finally, if the dispersion is due to the geometry of the structure, this type of mechanism appears as a slanted line with a negative slope. This style of behavior occurs for such structures such as waveguides where there exist different modes with different wave velocities as the frequency changes as seen in Figure 1.4e,f.

An example of the use of JTF processing in radar application is shown in Figure 1.5 where spectrogram of the simulated backscattered data from a dielectric-coated wire antenna is shown [14]. The backscattered field is collected from the Teflon-coated wire ($\varepsilon_r = 2.1$) such that the tip of the electric field makes an angle of 60° with the wire axis as illustrated in Figure 1.5. After the incident field hits the wire, infinitely successive scattering mechanisms occur. The first four of them are illustrated on top of Figure 1.5. The first return comes from the near tip of the wire. This event occurs at a discrete time that
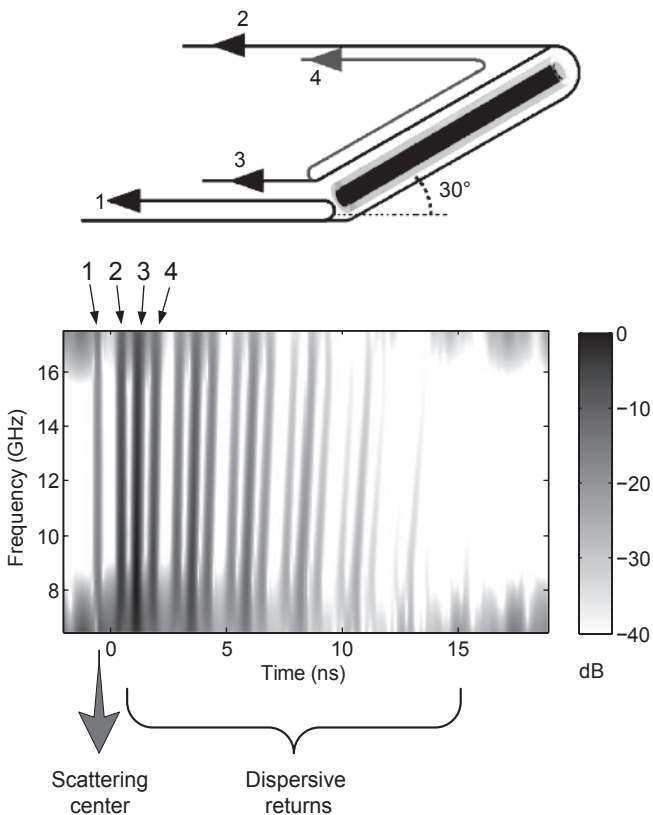

FIGURE 1.5   JTF image of a backscattered measured data from a dielectric-coated wire antenna using spectrogram.

exists at all frequencies. Therefore, this return demonstrates a scattering center-type mechanism. On the other hand, all other returns experience at least one trip along the dielectric-coated wire. Therefore, they confront a dispersive behavior. As the wave travels along the dielectric-coated wire, it is influenced by the dominant dispersive surface mode called Goubau [15]. Therefore, the wave velocity decreases as the frequency increases such that the dispersive returns are tilted to later times on the JTF plane. The dominant dispersive scattering mechanisms numbered 2, 3, and 4 are illustrated in Figure 1.5 where the spectrogram of the backscattered field is presented. The other dispersive returns with decreasing energy levels can also be easily observed from the spectrogram plot. As the wave travels on the dielectric-coated wire more and more, it is slanted more on the JTF plane, as expected.

1.4 CONVOLUTION AND MULTIPLICATION USING FT

Convolution and multiplication of signals are often used in radar signal processing. As listed in Equations 1.12 and 1.13, convolution is the inverse operation of multiplication as the FT is concerned, and vice versa. This useful feature of the FT is widely used in signal and image processing applications. It is obvious that the multiplication operation is significantly faster and easier to deal with when compared to the convolution operation, especially for long signals. Instead of directly convolving two signals in the time domain, therefore, it is much easier and faster to take the IFT of the multiplication of the spectrums of those signals as shown below:

$$
\begin{aligned}
g(t) * h(t) &= \mathcal{F}^{-1}\{\mathcal{F}\{g(t)\} \cdot \mathcal{F}\{h(t)\}\} \\
&= \mathcal{F}^{-1}\{G(f) \cdot H(f)\}.
\end{aligned}
\tag{1.18}
$$

In a dual manner, convolution between the frequency-domain signals can be calculated in a much faster and easier way by taking the FT of the product of their time-domain versions as formulated below:

$$
\begin{aligned}
G(f) * H(f) &= \mathcal{F}\{\mathcal{F}^{-1}\{G(f)\} \cdot \mathcal{F}^{-1}\{H(f)\}\} \\
&= \mathcal{F}\{g(t) \cdot h(t)\}.
\end{aligned}
\tag{1.19}
$$

1.5 FILTERING/WINDOWING

Filtering is the common procedure that is used to remove undesired parts of signals such as noise. It is also used to extract some useful features of the signals. The filtering function is usually in the form of a window in the frequency domain. Depending on the frequency inclusion of the window in the frequency axis, the filters are named low-pass (LP), high-pass (HP), or band-pass (BP).
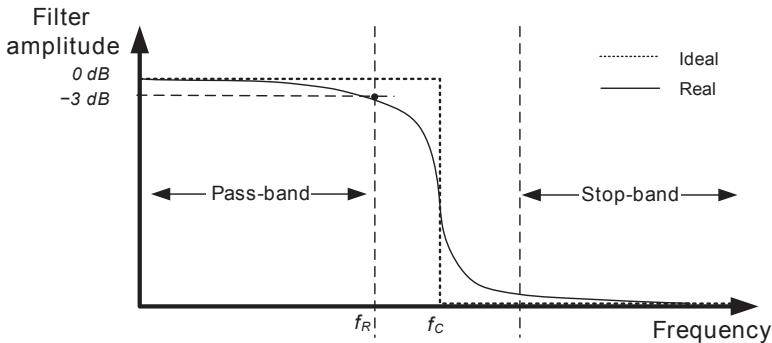
FIGURE 1.6   An ideal and real LP filter characteristics.

The frequency characteristics of an ideal LP filter are depicted as the dotted line in Figure 1.6. Ideally, this filter should pass frequencies from DC to the cutoff frequency of f_c and should stop higher frequencies beyond. In real practice, however, ideal LP filter characteristics cannot be realized. According to the Fourier theory, *a signal cannot be both time limited and band limited*. That is to say, to be able to achieve an ideal band-limited characteristic as in Figure 1.6, then the corresponding time-domain signal should theoretically extend from minus infinity to plus infinity which is of course impossible for realistic applications. Since all practical human-made signals are time limited, that is, they should start and stop at specific time instances, the frequency contents of these signals normally extend to infinity. Therefore, an ideal filter characteristic as the one in Figure 1.6 cannot be realizable, but only the approximate versions of it can be implemented in real applications. The best implementation of practical LP filter characteristic was achieved by Butterworth [16] and Chebyshev [17]. The solid line in Figure 1.6 demonstrates a real LP filter characteristic of Butterworth type.

Windowing procedure is usually applied to smooth a time-domain signal, therefore filtering out higher frequency components. Some of the popular windows that are widely used in signal and image processing are Kaiser, Hanning, Hamming, Blackman, and Gaussian. A comparative plot of some of these windows is given in Figure 1.7.

The effect of a windowing operation is illustrated in Figure 1.8. A time-domain signal of a rectangular window is shown in Figure 1.8a, and its FT is provided in Figure 1.8b. This function is in fact a *sinc* (*sinus cardinalis*) function and has major sidelobes. For the *sinc* function, the highest sidelobe is approximately 13 dB lower than the apex of the main lobe. This much of contrast, of course, may not be sufficient in some imaging applications. As shown in Figure 1.8c, the original rectangular time-domain signal is Hanning windowed. Its corresponding spectrum is depicted in Figure 1.8d where the sidelobes are highly suppressed, thanks to the windowing operation. For this example, the
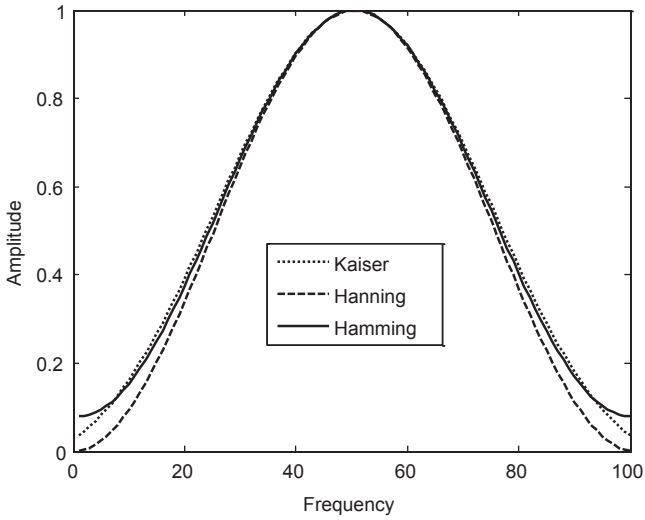
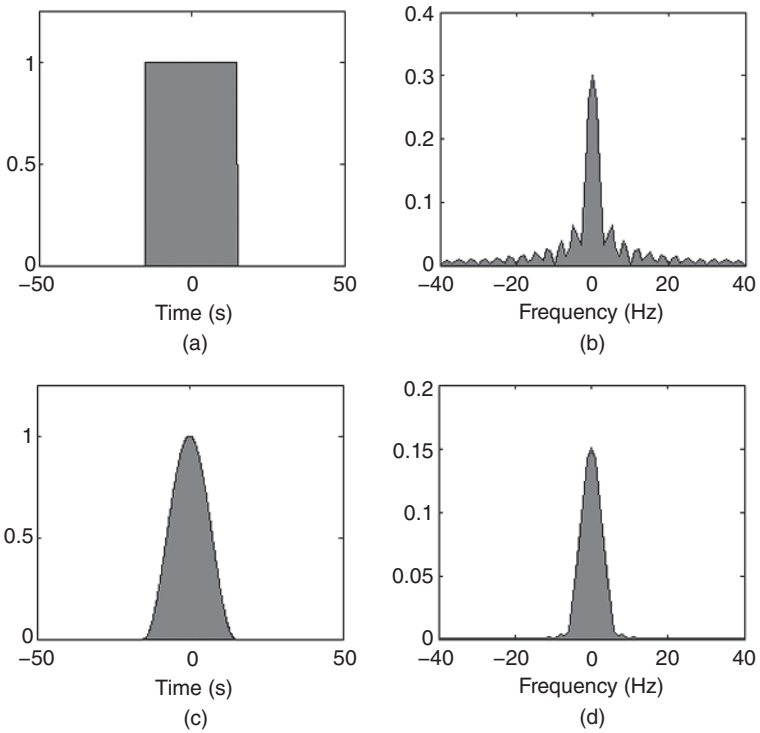**FIGURE 1.7**   Some common window characteristics.

FIGURE 1.8   Effect of windowing: (a) rectangular time signal, (b) its Fourier spectrum: a *sinc* signal, (c) Hanning windowed time signal, (d) corresponding frequency-domain signal.

highest sidelobe level is now 32 dB below the maximum value of the main lobe, which provides better contrast when compared to the original, nonwindowed signal.

A main drawback of windowing is the resolution decline in the frequency signal. The FT of the windowed signal has worse resolution than the FT of the original time domain signal. This feature can also be noticed from the example in Figure 1.8. By comparing the main lobes of the figures on the right, the resolution after windowing is almost twice as bad when compared to the original frequency domain signal. A comprehensive examination of windowing procedure will be presented later on, in Chapter 5.

1.6 DATA SAMPLING

Sampling can be regarded as the preprocess of transforming a continuous or analog signal to a discrete or digital signal. When the signal analysis has to be done using digital computers via numerical evaluations, continuous signals need to be converted to the digital versions. This is achieved by applying the common procedure of sampling. Analog-to-digital (A/D) converters are common electronic devices to accomplish this process. The implementation of a typical sampling process is shown in Figure 1.9. A time signal $s(t)$ is sampled at every T_s seconds such that the discrete signal, $s[n]$, is generated via the following equation:

$$s[n] = s(nT_s), \quad n = 0, 1, 2, 3, \dots \tag{1.20}$$

Therefore, the *sampling frequency*, f_s, is equal to $1/T_s$ where T_s is called the *sampling interval*.

A sampled signal can also be regarded as the digitized version of the multiplication of the continuous signal, $s(t)$, with the *impulse comb* waveform, $c(t)$, as depicted in Figure 1.10.

According to the Nyquist–Shannon sampling theorem, the perfect reconstruction of the signal is only possible provided that the sampling frequency, f_s, is equal to or larger than twice the maximum frequency content of the sampled signal [18]. Otherwise, signal aliasing is unavoidable, and only a distorted version of the original signal can be reconstructed.

1.7 DFT AND FFT

1.7.1 DFT

As explained in Section 1.1, the FT is used to transform continuous signals from one domain to another. It is usually used to describe the continuous
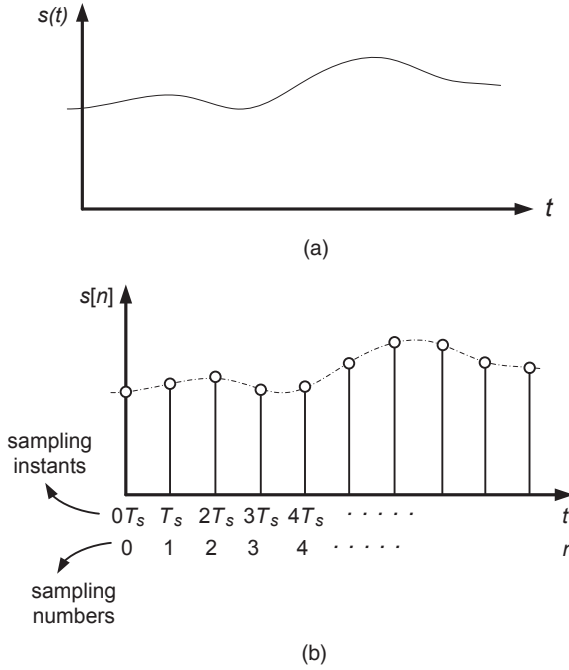
FIGURE 1.9   Sampling: (a) continuous time signal, (b) discrete time signal after the sampling.
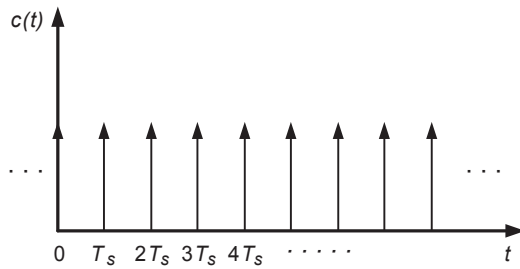

FIGURE 1.10   Impulse comb waveform composed of ideal impulses.

spectrum of an aperiodic time signal. To be able to utilize the FT while working with digital signals, the digital or DFT has to be used.

Let $s(t)$ be a continuous periodic time signal with a period of $T_o = 1/f_o$. Then, its sampled (or discrete) version is $s[n] \triangleq s(nTs)$ with a period of $NT_s = T_o$ where N is the number of samples in one period. Then, the Fourier integral in Equation 1.1 will turn to a summation as shown below:

$$S(kf_o) = \sum_{n=0}^{N-1} s(nT_s) \cdot e^{-j2\pi(kf_o)(nT_s)}$$

$$= \sum_{n=0}^{N-1} s(nT_s) \cdot e^{-j2\pi\left(\frac{k}{NT_s}\right)(nT_s)} \tag{1.21}$$

$$= \sum_{n=0}^{N-1} s(nT_s) \cdot e^{-j2\pi\frac{k}{N}n}.$$

Dropping the f_o and T_s inside the parenthesis for the simplicity of nomenclature and therefore switching to discrete notation, DFT of the discrete signal $s[n]$ can be written as

$$S[k] = \sum_{n=0}^{N-1} s[n] \cdot e^{-j2\pi\frac{n}{N}k} \tag{1.22}$$

In a dual manner, let $S(f)$ represent a continuous periodic frequency signal with a period of $Nf_o = N/T_o$ and let $s[k] \triangleq s(kf_o)$ be the sampled signal with the period of $Nf_o = f_s$. Then, the inverse discrete Fourier transform (IDFT) of the frequency signal $S[k]$ is given by

$$s\left(\frac{n}{f_s}\right) = \sum_{k=0}^{N-1} S(kf_o) \cdot e^{j2\pi(kf_o)\left(\frac{n}{f_s}\right)}$$

$$s(nT_s) = \sum_{k=0}^{N-1} S(kf_o) \cdot e^{j2\pi(kf_o)\left(\frac{n}{Nf_o}\right)} \tag{1.23}$$

$$= \sum_{k=0}^{N-1} S(kf_o) \cdot e^{j2\pi\frac{n}{N}k}.$$

Using the discrete notation by dropping the f_o and T_s inside the parenthesis, the IDFT of a discrete frequency signal $S[k]$ is given as

$$s[n] = \sum_{k=0}^{N-1} S[k] \cdot e^{j2\pi\frac{k}{N}n} \tag{1.24}$$

1.7.2   FFT

FFT is the efficient and fast way of evaluating the DFT of a signal. Normally, computing the DFT is in the order of N^2 arithmetic operations. On the other hand, fast algorithms like Cooley–Tukey's FFT technique produce arithmetic operations in the order of $N\log(N)$ [4, 19, 20]. An example of DFT is given in Figure 1.11 where a discrete time-domain ramp signal is plotted in Figure 1.11a, and its frequency-domain signal obtained by an FFT algorithm is given in Figure 1.11b.
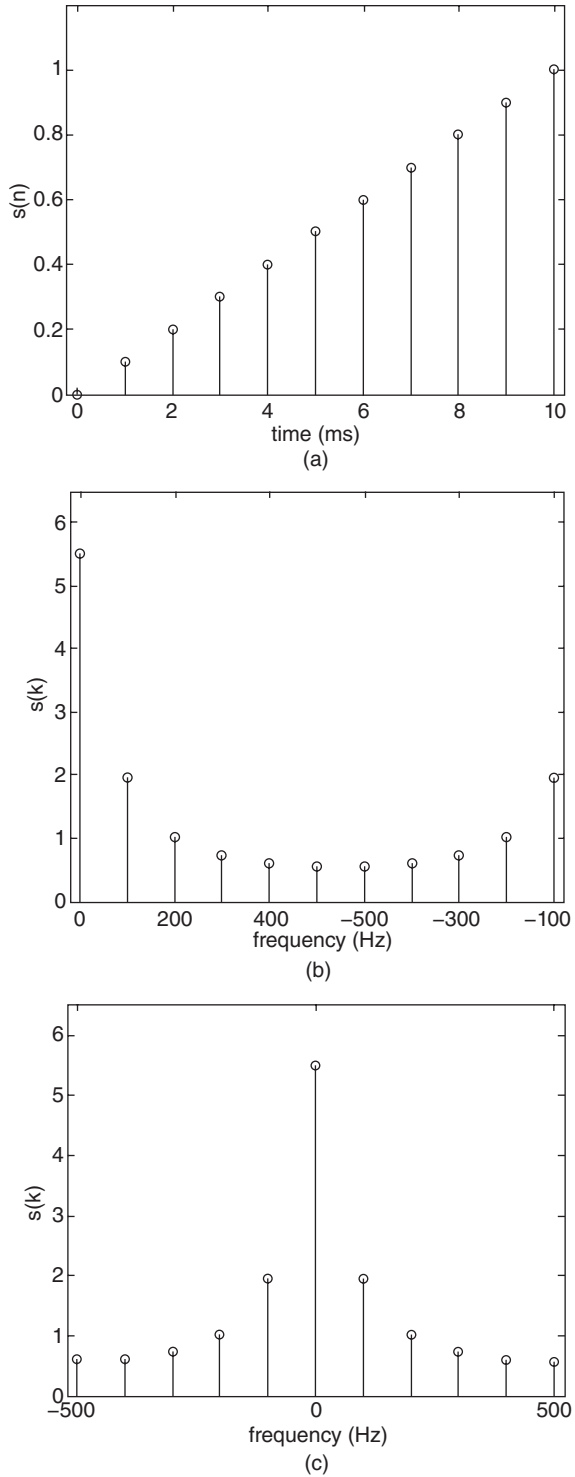
FIGURE 1.11 An example of DFT operation: (a) discrete time-domain signal, (b) discrete frequency-domain signal without FFT shifting, (c) discrete frequency-domain signal with FFT shifting.

1.7.3   Bandwidth and Resolutions

The duration, the bandwidth, and the resolution are important parameters while transforming signals from time domain to frequency domain or vice versa. Considering a discrete time-domain signal with a duration of $T_o = 1/f_o$ sampled N times with a sampling interval of $T_s = T_o/N$, the frequency resolution (or the sampling interval in frequency) after applying the DFT can be found as

$$\Delta f = \frac{1}{T_o}. \tag{1.25}$$

The spectral extend (or the frequency bandwidth) of the discrete frequency signal is

$$\begin{aligned} B &= N \cdot \Delta f \\ &= \frac{N}{T_o} \\ &= \frac{1}{T_s}. \end{aligned} \tag{1.26}$$

For the example in Figure 1.11, the signal duration is 1 ms with $N = 10$ samples. Therefore, the sampling interval is 0.1 ms. After applying the expressions in Equations 1.25 and 1.26, the frequency resolution is 100 Hz, and the frequency bandwidth is 1000 Hz. After taking the DFT of the discrete time-domain signal, the first entry of the discrete frequency signal corresponds to zero frequency, and negative frequencies are located in the second half of the discrete frequency signal as seen in Figure 1.11b. After the DFT operation, therefore, the entries of the discrete frequency signal should be swapped from the middle to be able to form the frequency axis correctly as shown in Figure 1.11c. This property of DFT will be thoroughly explored in Chapter 5 to demonstrate its use in inverse synthetic aperture radar (ISAR) imaging.

Similar arguments can be made for the case of IDFT. Considering a discrete frequency-domain signal with a bandwidth of B sampled N times with a sampling interval of Δf, the time resolution (or the sampling interval in time) after applying IDFT can be found as

$$\begin{aligned} \Delta t &= T_s \\ &= \frac{1}{B} \\ &= \frac{1}{N\Delta f}. \end{aligned} \tag{1.27}$$

The time duration of the discrete time signal is

$$T_o = \frac{1}{\Delta f}. \tag{1.28}$$

For the frequency-domain signal in Figure 1.11b or c, the frequency bandwidth is 1000 Hz with $N = 10$ samples. Therefore, the sampling interval in frequency is 100 Hz. After applying IDFT to get the time-domain signal as in Figure 1.11a, the formulas in Equations 1.27 and 1.28 calculate the resolution in time as 0.1 ms and the duration of the signal as 1 ms.

1.8   ALIASING

Aliasing is a type of signal distortion due to undersampling the signal of interest. According to Nyquist–Shannon sampling theorem [18], the sampling frequency, f_s, should be equal to or larger than twice the maximum frequency content, f_{max}, of the signal to be able to perfectly reconstruct the signal:

$$f_s \geq 2 f_{max}. \tag{1.29}$$

Since processing the analog radar signal requires sampling of the received data, the concept of aliasing should be taken into account when dealing with radar signals.

1.9   IMPORTANCE OF FT IN RADAR IMAGING

The imaging of a target using electromagnetic waves emitted from radars is mainly based on the phase information of the scattered waves from the target. This is because of the fact that the phase is directly related to the range distance of the target. In the case of monostatic radar configuration as shown in Figure 1.12a, let the scattering center on the target be at R distance away from the radar.

The scattered field E^s from this scattering center on the target has a complex scattering amplitude, A, and a phase factor that contains the distance information of the target as follows:

$$E^s(k) \cong A \cdot e^{-j2kR}. \tag{1.30}$$

As is obvious from Equation 1.30, there exists a Fourier relationship between the wave number, k, and the distance, R. Provided that the scattered field is collected over a bandwidth of frequencies (Fig. 1.12b), it is possible to pinpoint the distance R by Fourier transforming the scattered field data as depicted in Figure 1.12c. The plot of scattered field versus range is called the *range profile*, which is an important phenomenon in radar imaging. Range profile is in
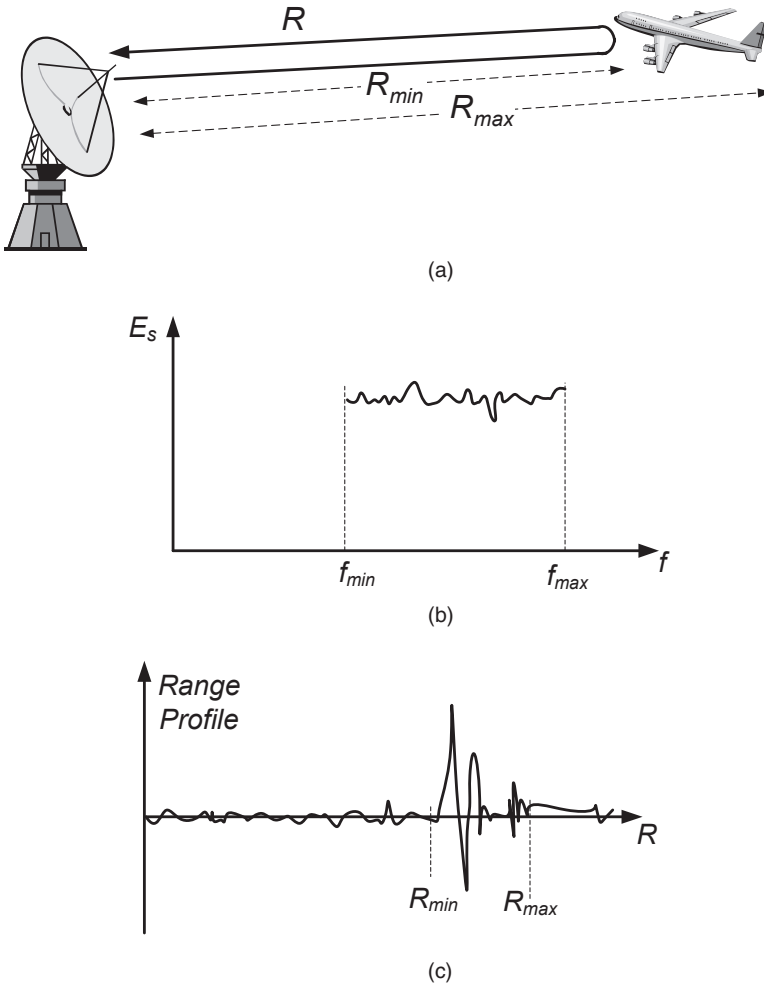
(a)

(b)

(c)

FIGURE 1.12   (a) Monostatic radar configuration, (b) scattered field versus frequency, (c) range profile of the target.

fact nothing but the one-dimensional range image of the target. An example is illustrated in Figure 1.13 where the range profile of an airplane is shown. The concept of range profiling will be thoroughly investigated in Chapter 4, Section 4.3.

Another main usage of FT in radar imaging is the ISAR imaging. In fact, ISAR can be regarded as the 2D range and cross-range profile image of a target. While the range resolution is achieved by utilizing the frequency diversity of the backscattered signal, the cross-range resolution is gathered by collecting the backscattered signal over different look angles of the target. An example of ISAR imaging for the same airplane is demonstrated in Figure
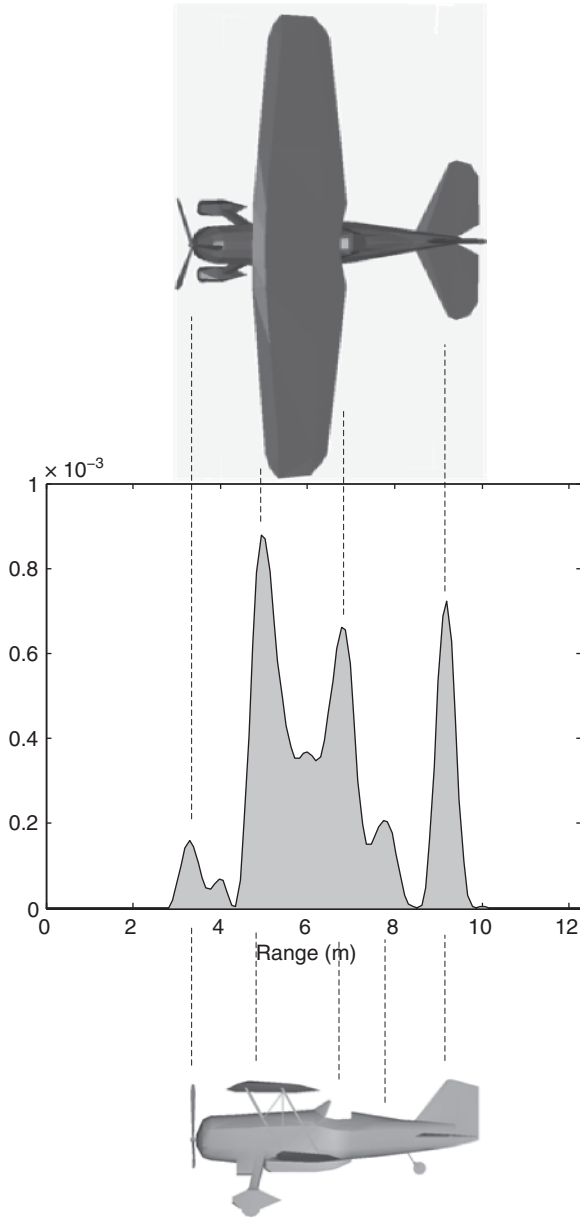
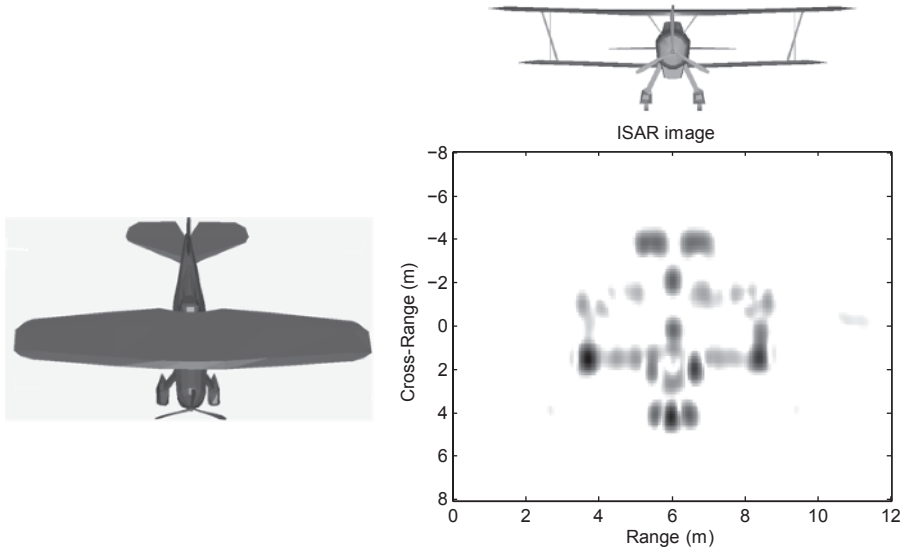**FIGURE 1.13**   Simulated range profile of an airplane.

FIGURE 1.14   Simulated two-dimensional ISAR image of an airplane.

1.14 where both the CAD view and the constructed ISAR image for the airplane is shown. The concept of ISAR imaging will be examined in great detail in Chapter 4.

The FT operations are also extensively used in synthetic aperture radar (SAR) imaging as well. Since the SAR data are usually huge and processing this amount of data is an extensive and time-consuming task, the FTs are usually utilized to achieve both range and azimuth compression procedures.

An example of SAR imagery is given in Figure 1.15 where the image was acquired by spaceborne imaging radar-C/X-band synthetic aperture radar (SIR-C/X-SAR) onboard the space shuttle Endeavour in 1994 [21]. This SAR image covers an area of Cape Cod, Massachusetts. The details of SAR imagery will be explored in Chapter 3.

1.10   EFFECT OF ALIASING IN RADAR IMAGING

In radar applications, the data are collected within a finite bandwidth of frequencies. According to the sampling theory, if the radar signal is $g(t)$ and its spectrum is $G(f)$, and the frequency components beyond a specific frequency B are zero, that is,

$$G(f) = \begin{cases} \neq 0 & ; |f| < B \\ 0 & ; |f| \geq B, \end{cases} \tag{1.31}$$
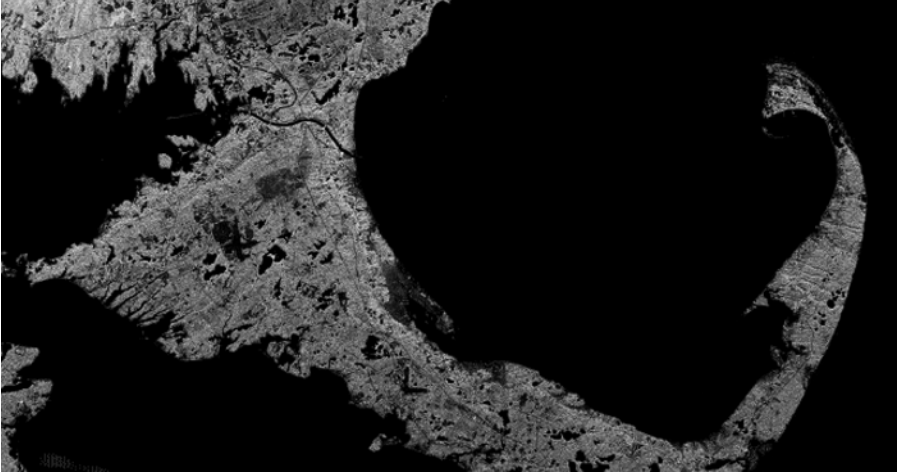
FIGURE 1.15   SAR image of the famous "hook" of Cape Cod, Massachusetts, USA [21].

then the time-domain signal $g(t)$ should be sampled at least twice the bandwidth in frequency as

$$f_s = 2B, \tag{1.32}$$

where f_s stands for the sampling frequency.

When the radar imaging is concerned, the scattered electric field has the form as given in Equation 1.30. The sampling theorem can be applied in the following manner:

Suppose that target to be imaged lies in the range direction within the range width or range extend of R_{max} such that

$$-\frac{R_{max}}{2} \le r \le \frac{R_{max}}{2} \tag{1.33}$$

as depicted in Figure 1.16b. In the case of imaging radar, this figure represents the range profile of the target. The FT of $g(r)$ represents its spectrum that theoretically extends to infinity in the frequency axis (see Fig. 1.16a). The main problem is to get the digitized (or sampled) versions of $g(r)$ from digitized (or sampled) versions of $G(k)$ or $G(f)$ with adequate samples so that no aliasing occurs. Here, k stands for the wave number and is related to the operating frequency as

$$k = 2\pi f/c \tag{1.34}$$
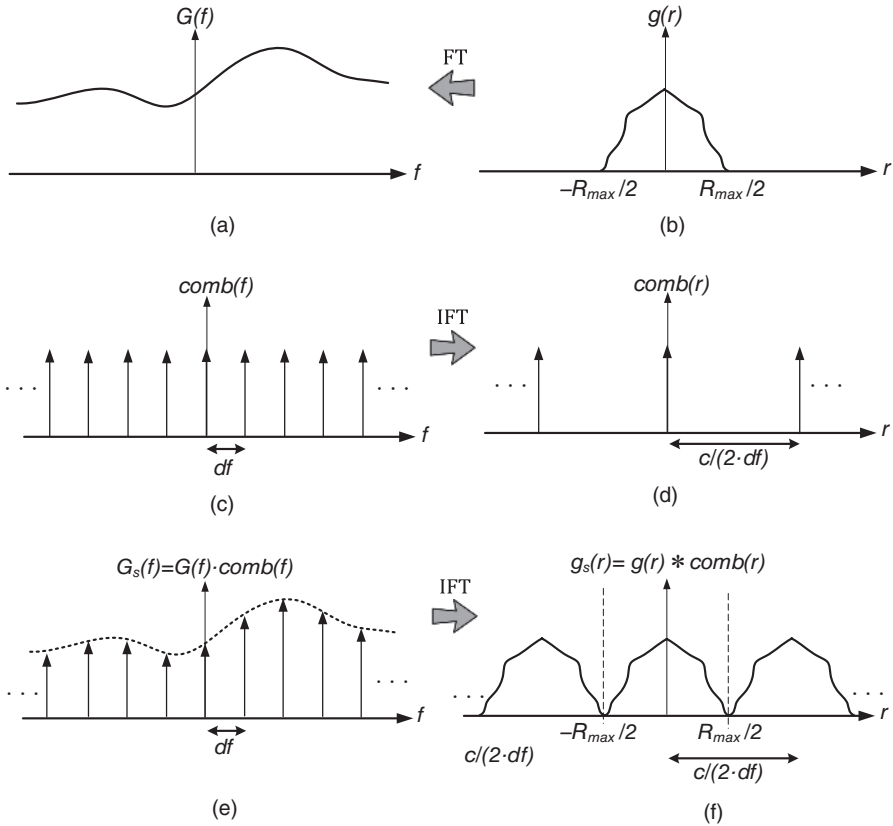
FIGURE 1.16 The Nyquist sampling procedure for getting unaliased range image: (a) frequency-domain radar signal for a range windowed data, (b) range domain signal, (c) sampling comb signal in frequency domain, (d) its range domain equivalent, (e) critically sampled version of the frequency-domain signal, and (f) its range domain equivalent.

where c is the speed of light. Utilizing the relationship between the wave number, k, and the distance, R, in Equation 1.30, the sampling in the wave-number domain should satisfy the following inequality:

$$dk \leq \frac{2\pi}{2R_{max}}$$
$$= \frac{\pi}{R_{max}}. \tag{1.35}$$

This inequality is forced by the famous Nyquist sampling condition. The minimum sampling frequency, then, should be equal to

$$(df)_{min} = \frac{c}{2\pi}(dk)_{min}$$

$$= \frac{c}{2\pi} \cdot \frac{\pi}{R_{max}} \tag{1.36}$$

$$= \frac{c}{2R_{max}}.$$

Then, the sampled version of frequency-domain signal $G(f)$ is obtained by the multiplication of the $G(f)$ with the following impulse comb function:

$$comb(f) = \sum_n \delta(f - n \cdot df). \tag{1.37}$$

The plot of this comb function is shown in Figure 1.16c. By taking the IFT of this comb function, we can get another comb function in the range domain as

$$comb(r) = \mathcal{F}^{-1}\{comb(f)\}$$
$$= \mathcal{F}^{-1}\left\{\sum_n \delta(f - n \cdot df)\right\} \tag{1.38}$$
$$= \frac{c}{2df}\sum_n \delta\left(r - n \cdot \frac{c}{2df}\right)$$

as depicted in Figure 1.16d. The sampled version of frequency-domain signal, $G_s(f)$, can be obtained by multiplying the original frequency-domain signal, $G(f)$, with the impulse comb function in Figure 1.16c as

$$G_s(f) = G(f) \cdot comb(f)$$
$$= \sum_n G(f) \cdot \delta(f - n \cdot df), \tag{1.39}$$

which is shown in Figure 1.16e. The range domain equivalent of the frequency-domain sampled signal can be found via inverse Fourier transformation as

$$g_s(r) = \mathcal{F}^{-1}\{G_s(f)\}$$
$$= \mathcal{F}^{-1}\{G(f) \cdot comb(f)\}$$
$$= g(r) * comb(r)$$
$$= g(r) * \frac{c}{2df}\sum_n \delta\left(r - n \cdot \frac{c}{2df}\right) \tag{1.40}$$
$$= \frac{c}{2df}\sum_n g\left(r - n \cdot \frac{c}{2df}\right),$$

where "*" is the convolution operation. Therefore, the resultant range domain signal is periodic with $(c/2df)$ intervals. If df is chosen to be equal to
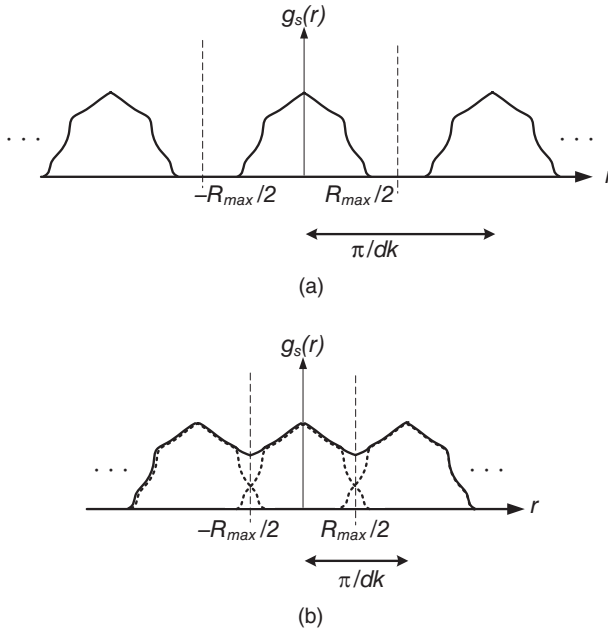
FIGURE 1.17   The effect of sampling rate: (a) no aliasing due to oversampling and (b) aliased or distorted range domain waveform due to undersampling.

$(df)_{min} = c/2R_{max}$, the period of $g_s(r)$ becomes R_{max} as illustrated in Figure 1.16f. If $G(f)$ is sampled and found to be finer than $(df)_{min}$, that is, over-sampled, no aliasing occurs, and the resultant $g_s(r)$ signal will be similar to the one in Figure 1.17a. Therefore, when the DFT is used, the original range domain signal falls within one period of $g_s(r)$ and can be recovered without any distortion. When a sampling rate of $df \geq (df)_{min}$ is used, $g_s(r)$ signal is aliased as demonstrated in Figure 1.17b, and the original range domain signal $g(r)$ is distorted within one period of $(c/2df)$. Therefore, the recovery of $g(r)$ is not possible due to undersampling of $G(f)$. The effect of aliasing in ISAR imaging will be covered in Chapter 5, Section 5.2.

1.11   MATLAB CODES

Below are the Matlab source codes that were used to generate all of the Matlab-produced Figures in Chapter 1. The codes are also provided in the CD that accompanies this book.

Matlab code 1.1: Matlab file "Figure1-1.m"

```
%-------------------------------------------------------------
% This code can be used to generate Figure 1_1
```

```
%------------------------------------------------------------
% This file requires the following files to be present in the
same
% directory:
%
%prince.wav

clear all
close all

% Read the sound signal "prince.wav"
[y,Fs,bits] = wavread('prince.wav');
sound(y,Fs);
N = length(y);

% TIME DOMAIN SIGNAL
t = 0:.8/(N-1):.8;
plot(t,y,'k'); %downsample for plotting
set(gca,'FontName', 'Arial', 'FontSize',14,'FontWeight','Bold');
axis tight;
xlabel('Time [s]');
ylabel('Amplitude');
title('time domain signal');
```

Matlab code 1.2: Matlab file "Figure1-2.m"
```
%------------------------------------------------------------
% This code can be used to generate Figure 1.2
%------------------------------------------------------------
% This file requires the following files to be present in the
same
% directory:
%
%prince.wav

clear all
close all

% Read the sound signal "prince.wav"
[y,Fs,bits] = wavread('prince.wav');
sound(y,Fs); %play the sound
N = length(y);

t = 0:.8/(N-1):.8; %form time vector

% FREQUENCY DOMAIN SIGNAL
Y = fft(y)/N;
% Calculate the spectrum of the signal
df = 1/(max(t)-min(t)); % Find the resolution in frequency
f = 0:df:df*(length(t)-1); % Form the frequency vector
```

```
plot(f(1:2:N),abs(Y(1:(N+1)/2)),'k') %downsample for plotting
set(gca,'FontName', 'Arial', 'FontSize',14,'FontWeight','Bold');
axis tight;
xlabel('Frequency [Hz]');
ylabel('Amplitude');
title('frequency domain signal');
```

Matlab code 1.3: Matlab file "Figure1-3.m"
```
%-------------------------------------------------------------
% This code can be used to generate Figure 1.3
%-------------------------------------------------------------
% This file requires the following files to be present in the
same
% directory:
%
%prince.wav

clear all
close all

% Read the sound signal "prince.wav"
[y,Fs,bits] = wavread('prince.wav');
sound(y,Fs);
N = length(y);

t = 0:.8/(N-1):.8; %form time vector

% TIME FREQUENCY PLANE SIGNAL
A = spectrogram(y,256,250,400,1e4); % Calculate the
spectrogram
matplot(t,f, (abs(A)),30); % Display the signal in T-F
domain
colormap(1-gray); % Change the colormap to grayscale
set(gca,'FontName', 'Arial', 'FontSize',14,'FontWeight','Bold');
xlabel('Time [s]');
ylabel('Frequency [Hz]');
title('signal in time-frequency plane');
```

Matlab code 1.4: Matlab file "Figure1-5.m"
```
%-------------------------------------------------------------
% This code can be used to generate Figure 1.5
%-------------------------------------------------------------
% This file requires the following files to be present in the
same
% directory:
%
% tot30.mat
clear all
close all
```

```
load tot30; % load the measured back-scattered E-field

% DEFINITION OF PARAMETERS
f = linspace(6,18,251)*1e9; %Form frequency vector
BW = 6e9; % Select the frequency window size
d = 2e-9; %Select the time delay

% DISPLAY THE FIELD IN JTF PLANE
[B,T,F] = stft(tot30,f,BW,50,d);
xlabel('--->Time (nsec)');
ylabel('--> Freq. (GHz)');
colorbar;
colormap(1-gray)
set(gca,'FontName', 'Arial', 'FontSize',14,'FontWeight','Bold
');
axis tight;
xlabel('Time [ns]');
ylabel('Frequency [GHz]');
```

Matlab code 1.5: Matlab file "Figure1-8.m"

```
%----------------------------------------------------------------
% This code can be used to generate Figure 1.8
%----------------------------------------------------------------

clear all
close all

%% DEFINE PARAMETERS
t = linspace(-50,50,1001); % Form time vector
df = 1/(t(2)-t(1)); %Find frequency resolution
f = df*linspace(-50,50,1001);% Form frequency vector

%% FORM AND PLOT RECTANGULAR WINDOW
b(350:650) = ones(1,301);
b(1001) = 0;
subplot(221);
h = area(t,b);
set(gca,'FontName', 'Arial', 'FontSize',14,'FontWeight','Bold
');
xlabel('Time [s]');
axis([-50 50 0 1.25])
set(h,'FaceColor',[.5 .5 .5])

subplot(222);
h = area(f,fftshift(abs(ifft(b))));
set(gca,'FontName', 'Arial', 'FontSize',14,'FontWeight','Bold
');
xlabel('Frequency [Hz]')
axis([-40 40 0 .4])
```

```
set(h,'FaceColor',[.5 .5 .5])

%% FORM AND PLOT HANNING WINDOW
bb = b;
bb(350:650) = hanning(301)';

subplot(223);
h = area(t,bb);
set(gca,'FontName', 'Arial', 'FontSize',14,'FontWeight','Bold
');
xlabel('Time [s]');
axis([-50 50 0 1.25])
set(h,'FaceColor',[.5 .5 .5])

subplot(224);
h = area(f,fftshift(abs(ifft(bb))));
set(gca,'FontName', 'Arial', 'FontSize',14,'FontWeight','Bold
');
xlabel('Frequency [Hz]')
axis([-40 40 0 .2])
set(h,'FaceColor',[.5 .5 .5])
```

Matlab code 1.6: Matlab file "Figure1-11.m"
```
%------------------------------------------------------------
% This code can be used to generate Figure 1.11
%------------------------------------------------------------
clear all
close all

%--- Figure 1.11(a)------------------------------------------
% TIME DOMAIN SIGNAL
a = 0:.1:1;
t = (0:10)*1e-3;
stem(t*1e3,a,'k','Linewidth',2);
set(gca,'FontName', 'Arial', 'FontSize',14,'FontWeight','Bold
');
xlabel('time [ms]'); ylabel('s[n]');axis([-0.2 10.2 0 1.2]);

% FREQUENCY DOMAIN SIGNAL
b = fft(a);
df = 1./(t(11)-t(1));
f = (0:10)*df;
ff = (-5:5)*df;
%--- Figure 1.11(b)------------------------------------------
Figure;
stem(f,abs(b),'k','Linewidth',2);
set(gca,'FontName', 'Arial', 'FontSize',14,'FontWeight','Bold
');
```

```
xlabel('frequency [Hz]'); ylabel('S[k]');axis([-20 1020 0
6.5]);
set(gca,'FontName', 'Arial', 'FontSize',12,'FontWeight',
'Bold');

%--- Figure 1.11(c)---------------------------------------------
Figure;
stem(ff,fftshift(abs(b)),'k','Linewidth',2);
set(gca,'FontName', 'Arial', 'FontSize',14,'FontWeight','Bold
');
xlabel('frequency [Hz]'); ylabel('S[k]');axis([-520 520 0
6.5]);
set(gca,'FontName', 'Arial', 'FontSize',12,'FontWeight',
'Bold');
```

REFERENCES

1 J. Fourier. *The analytical theory of heat*. Dover Publications, New York, 1955.
2 C. Runge. *Zeit für Math und Physik* 48 (1903) 433.
3 G. C. Danielson and C. Lanczos. Some improvements in practical Fourier analysis and their application to X-ray scattering from liquids. *J Franklin Inst* 233 (1942) 365.
4 J. W. Cooley and J. W. Tukey. An algorithm for the machine calculation of complex Fourier series. *Math Comput* 19 (1965) 297–301.
5 From http://www.ling.ohio-state.edu/~cclopper/courses/prince.wav (accessed at 08.10.2007).
6 J. B. Allen. Short term spectral analysis, synthesis, and modification by discrete Fourier transform. *IEEE Trans Acoust* ASSP-25 (1977) 235–238.
7 A. T. Nuttall. Wigner distribution function: Relation to short-term spectral estimation, smoothing, and performance in noise, Technical Report 8225, Naval Underwater Systems Center, 1988.
8 L. Du and G. Su. Target number detection based on a order Choi-Willams distribution, signal processing and its applications. Proceedings, Seventh International Symposium on Volume 1, Issue, 1–4 July 2003, pp. 317–320, vol.1, 2003.
9 L. Cohen. Time frequency distribution—A review. *Proc IEEE* 77(7) (1989) 941–981.
10 S. Qian and D. Chen. *Joint time-frequency analysis: Methods and applications*. Prentice Hall, New Jersey, 1996.
11 V. C. Chen and H. Ling. *Time-frequency transforms for radar imaging and signal processing*. Artech House, Norwood, MA, 2002.
12 L. C. Trintinalia and H. Ling. Interpretation of scattering phenomenology in slotted waveguide structures via time-frequency processing. *IEEE Trans Antennas Propagat* 43 (1995) 1253–1261.
13 A. Filindras, U. O. Larsen, and H. Ling. Scattering from the EMCC dielectric slabs: Simulation and phenomenology interpretation. *J Electromag Waves Appl* 10 (1996) 515–535.

14   C. Özdemir and H. Ling. Joint time-frequency interpretation of scattering phe-nomenology in dielectric-coated wires. *IEEE Trans Antennas Propagat* 45(8) (1997) 1259–1264.

15   J. H. Richmond and E. H. Newman. Dielectric-coated wire antennas. *Radio Sci* 11 (1976) 13–20.

16   R. W. Daniels. *Approximation methods for electronic filter design*. McGraw-Hill, New York, 1974.

17   A. B. Williams and F. J. Taylors. *Electronic filter design handbook*. McGraw-Hill, New York, 1988.

18   C. E. Shannon. Communication in the presence of noise. *Proc Inst Radio Eng* 37(1) (1949) 10–21.

19   N. Brenner and C. Rader. A new principle for fast Fourier transformation. *IEEE Trans Acoust* 24 (1976) 264–266.

20   P. Duhamel. Algorithms meeting the lower bounds on the multiplicative complex-ity of length-2n DFTs and their connection with practical algorithms. *IEEE Trans Acoust* 38 (1990) 1504–1511.

21   From internet, http://www.jpl.nasa.gov/radar/sircxsar/capecod2.html (accessed at 01.07.2008).